

MULTIPHASE FLOW INVESTIGATION OF A CENTRIFUGAL FILTER USING COMPUTATIONAL FLUID DYNAMICS AND EXPERIMENTS

Steven D Megson
Department of Mechanical
Engineering
University of Bath
Bath BA2 7 AY, UK

Michael Wilson
Department of Mechanical
Engineering
University of Bath
Bath BA2 7 AY, UK

Stuart A MacGregor
Department of Mechanical
Engineering
University of Bath
Bath BA2 7 AY, UK

ABSTRACT

Modern "high tech" lubricant oils have been developed to contain a high level of dispersant additive to the base oil. As contaminant loading has increased, designers are required to address the problem of controlling the contamination found in the oil. One method is the use of bypass centrifugal sedimentation. This paper describes a computational study of the basic flow characteristics in a centrifugal sedimenting rotor using the computational fluid dynamics (CFD) package STAR-CD.

Simplified CFD models have indicated regions of flow which would be difficult to demonstrate by experimental methods alone. For example, backflow from the outlet channel is found to cause a disruptive secondary flow in some models, but this flow is contained by the inclusion of a more realistic geometry. Two-phase flow computations have also been carried out to investigate the behaviour of spherical particulates of different sizes. Flow and geometry factors affecting the centrifuge performance are discussed.

INTRODUCTION

Modern "high tech" lubricant oils have been developed to contain a high level of dispersant additive to the base oil. However as contaminant loading has increased to unprecedented levels, with the introduction of EGR and other design changes, to enable diesel engines to meet environmental legislation, it is questionable how much further

oil development has in reserve for future emissions clampdowns. Designers are therefore required to address the problem of controlling the contamination found in the lube oil.

A general method used for reducing the amount of contaminant in the lube oil is to remove some of it by filtration [1], which indeed engines have been using for many years. The problem when dealing with combustion debris is one of size; research has shown soot particles, which are the prime particulate contaminant found in diesel lube oil, to be sized between 20–30nm [1–5] for primary particles and 0.2–0.3 μ m for the larger aggregates [1,5–8]. The size of the contaminant particulate means that traditional barrier media would require an unacceptably large filter to overcome losses and plugging.

One method of controlling the lube oil contaminant is by the use of bypass centrifugal sedimenting oil cleaners, which has proved to be effective in contaminant removal thus extending lube oil life and therefore extending engine life. Separation by centrifugal phenomena is based on the transfer of materials from one phase to another by mechanical means utilising differences in particle density and size in mixtures under an applied centrifugal force field [9], and can ultimately separate particles sized to the sub micron range.

Centrifugal sedimenting oil cleaners have another distinct advantage over media bypass filtration methods in that cleaning efficiency remains virtually constant over their life as there is no media barrier to block or bypass valve to open [6].



Figure 1. A (MANN+HUMMEL) Centrifugal Sedimenting Oil Cleaning Rotor

The study of centrifugal sedimentation within the filtration industry is limited [6]. Centrifugal separation includes both motor-driven and self-driven centrifuges which are subtly different in both design and operation. Most papers that have been presented on centrifugal separation mainly cover motor driven centrifuges which tend to be large and expensive units, having extensive applications in process industries and very large marine diesel engines for the cleaning of both fuel and lubricating oils [6]. Self-driven centrifuges tend to be much smaller, with the main area of application being medium to high speed diesel engine lubrication systems.

This paper describes a CFD study undertaken to model the flow characteristics in a self-driven centrifugal sedimenting rotor, in order to gain a fundamental understanding of the flows and effects of different geometric features. Although the first model (see Figure 2) was simple in construction, a sequence of models of increasing geometric complexity has been considered.

Complementing and running in parallel with the computational work, flow visualisation experiments are also being carried out to verify the computations and increase the understanding of results. This increases knowledge of the flow field present in the system and demonstrates how changes in the geometry of the rotor affect the flow.

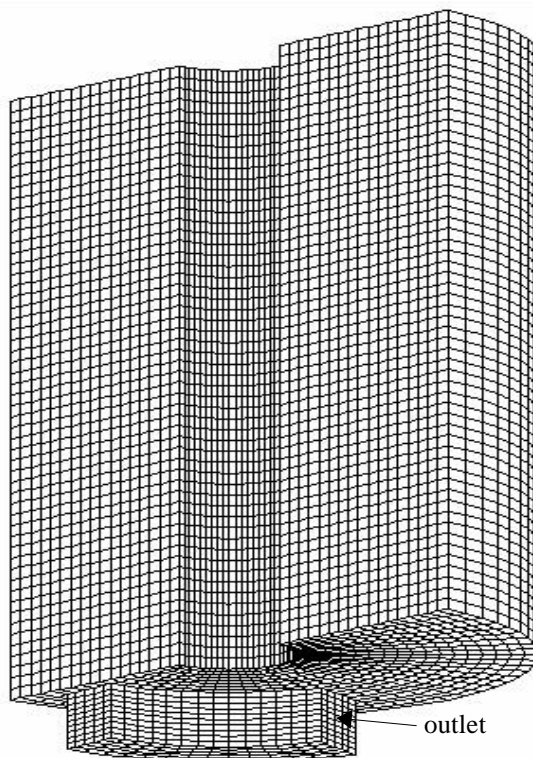


Figure 2. The Basic Model

DESCRIPTION OF THE CENTRIFUGAL SEDIMENTING ROTOR

Self powered oil cleaning centrifuges are typically used in bypass processing. Approximately 10% of the lube oil is pumped by the engine oil pump and enters a hollow spindle (Figure 3) on which the rotor is supported.

The oil exits via a cross hole into the transfer chamber (Figure 4) between the spindle and inner casing of the rotor, and is in direct contact with the bearings. The oil exits the transfer chamber radially via the centrifuge rotor inlets which again consist of a cross through drilling. The rotor becomes full of pressurised oil which exits via two tangentially opposed outlet nozzles in the rotor base. The energy produced by the outlet jets causes rotation of the self driven free spinning rotor assembly (similar in principle to that of a garden sprinkler). The oil in the rotor accelerates up to the same rotational speed as the rotor.



Figure 3. The Hollow Spindle

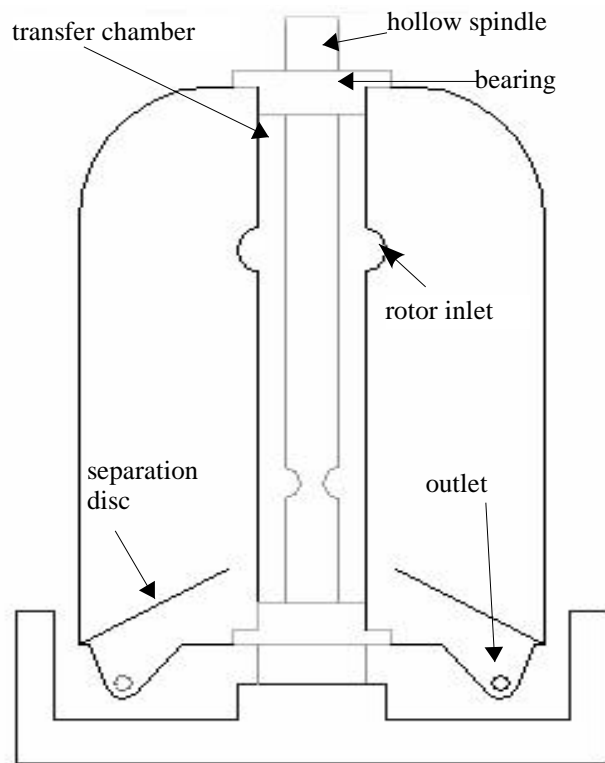


Figure 4. The Centrifuge Assembly

When the contaminant particles carried by the lube oil enter the rotor they are therefore subjected to a centrifugal force. Particles of greater density than the lube oil are deposited on the interior surface of the outer wall by centrifugal sedimentation. The oil exits via the two outlets in the rotor base back to the sump whilst the sedimented particles are retained as a "cake" on the inner surface of the rotor's outer wall (Figure 5).

The expected behaviour of a solid particle in the centrifugal force field can be estimated by considering the equation of motion for the radial component V_r of the particle velocity at any radial location r [9]:

$$\frac{dV_r}{dt} = (1 - \bar{\rho}) r \omega^2 - \frac{3}{4} C_D \frac{\bar{\rho} V_r^2}{D_p} \quad (1)$$

Where $\bar{\rho} = \rho_f / \rho_p$, ρ_f is the fluid density, ρ_p is the density of the particle, ω is its angular velocity and D_p is the particle diameter. This radial velocity is constant with time when $dV_r/dt = 0$, i.e. when

$$V_r^2 = \frac{(1 - \bar{\rho})}{\bar{\rho}} r \omega^2 \frac{4D_p}{3C_D} \quad (2)$$

If the Reynolds number for the flow over the particle is sufficiently low the drag coefficient C_D can be given by Stokes Law:

$$C_D = \frac{24}{Re} \quad (\text{when } Re = \frac{\rho_f V_r D_p}{\mu} < 0.4) \quad (3)$$

Equation (2) then becomes,

$$V_r = \frac{(\rho_p - \rho_f) r \omega^2 D_p^2}{18 \mu} \quad (4)$$

For fixed operating conditions the density difference $(\rho_p - \rho_f)$ is fixed. Equation (4) shows that the radial (outward) velocity of a particle will increase with increasing ω and with increasing D_p , i.e. high rotation rates and large particle sizes will give rise to more effective centrifuge behaviour.

For the study described here the fluid (oil) properties were taken as $\rho_f = 845 \text{ kg/m}^3$ and $\mu = 0.01479 \text{ kg/ms}$. A density of $\rho_p = 2000 \text{ kg/m}^3$ was estimated for the particle contaminant. The rotor outer radius is $b = 0.044 \text{ m}$; normal operating conditions are a rotational speed of 6800 rpm at a flow-rate of 6.2 litres/min. These values give a Reynolds number (using equation (3)) within the Stokes Law range for the largest particle size studied here ($D_p = 3 \times 10^{-5} \text{ m}$) at the outer radius of the rotor.

The ratio Z of the centrifugal to the gravitational force is a measure of the separating power of the centrifuge. The value of Z for the rotor at the above operating speed is 2274 at the outer radius.

A radial Reynolds number for the fluid at the inlet nozzles at the design flow-rate is,

$$Re_r = \frac{\rho_f V_r b}{\mu} = 2067 \quad (5)$$

The corresponding rotational Reynolds number is,

$$Re_\phi = \frac{\rho_f \omega b^2}{\mu} = 78,764 \quad (6)$$

The sedimenting oil centrifuge is capable of removing a wide range of particulate contaminant sizes, extending into the sub-micron range [10]. A full flow barrier filter that was capable of trapping particulate contaminant of the sub-micron size would prove unworkable due to the size needed to overcome the losses of pressure and flow that would occur as a result of clogging. This highlights one of the many benefits of using a bypass sedimenting oil centrifuge.

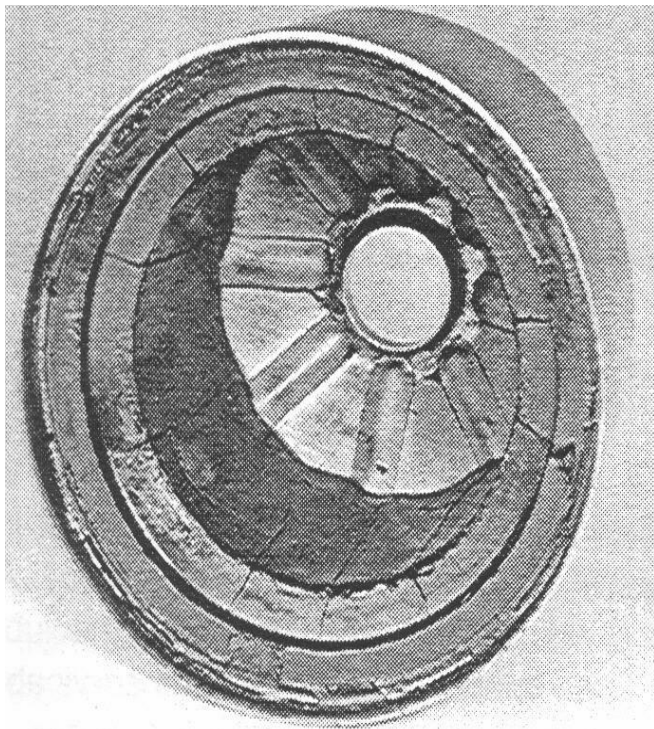


Figure 5. Inside the Cleaning Chamber of a Straight-Ribbed Rotor with Contaminant Cake [12]

COMPUTATIONAL MODEL

The flow characteristics within the centrifuge were analysed in stages in order to gain a better understanding of the effects of different flows and geometric features. The general purpose CFD software STAR-CD was used for the computational studies.

Due to symmetry, half of the rotor was modelled and cyclic symmetry conditions imposed at the tangential boundaries at 0 and 180 degrees, so that fluid leaving through one face re-enters at the corresponding point on the other boundary (This condition was not applied at the outlet channel).

The inlet is positioned at the inner spindle which forms the axis of rotation; the small outlet is positioned on the tangential face of the outlet channel (see Figures 1,2), and a rotational reference frame is used to simulate the rotation of the filter rotor at a prescribed rotation rate (ω).

Figure 1 shows the model used in initial computations, which was run without rotation but with inlet and outlet flow. The other extreme condition, with the rotor rotating at its operating speed but with no flow at the inlet and outlet was also computed. Subsequently, the combined flow fields were computed. This model gave a good indication of how the operating conditions affected the flow field and provided a datum for increasing the geometric complexity of the models.

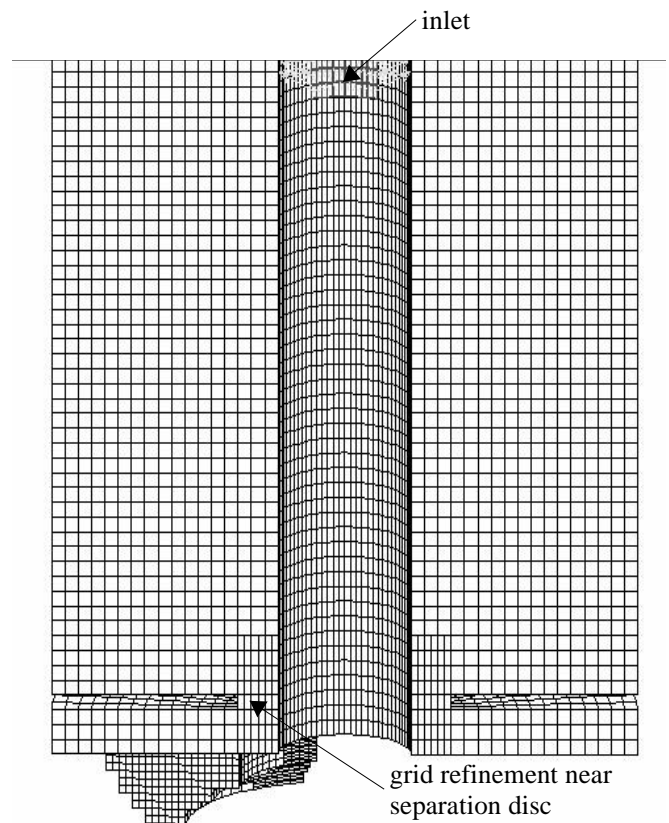


Figure 6. The Separation Disc

The separation disc was the first additional feature to be included in the computational mesh. The separation disc provides the rotor with two chambers, a large upper chamber and a much smaller lower chamber as shown in Figure 4. Its function within the centrifugal sedimenter is to prevent the cake that has settled against the outer wall from slumping down within the rotor.

Local grid refinements were necessary in the region that links the two chambers and also in the outlet channel (see Figure 6), as gradients in the flow properties were expected to be significant in these areas. This model had a total of 40,644 computational cells. The models were run at the normal operating conditions of 6.2 litres/min flowrate and rotational speed of 6800rpm.

Turbulence was represented using an isotropic $k-\epsilon$ turbulence model with wall functions [11]. Despite the known deficiencies of this model for some swirling flows, other computations carried out using anisotropic variants gave results in good agreement with the more computationally efficient isotropic model. In the present study, this may be due to the presence of only relatively small departures from solid body rotation in the filter flow-field. A multidimensional second order accurate differencing scheme, MARS [11], not relying on any problem dependent parameters, was used for all of the 3D flow computations described here. Further grid refinement tests showed the results presented not to depend significantly on the mesh resolution used.

In addition to solving the (finite volume forms of) the transport equations for the continuous fluid, STAR-CD can also be used to solve Lagrangian equations of motion for a discontinuous solid phase dispersed within the fluid [11]. The dispersed phase is included in the model by defining the initial position, velocity, size and density of the individual dispersed phase elements (the contaminant particles in this work). (The Lagrangian equation takes the form of equation (1) when the particles rotate with the same angular velocity as the fluid.)

The computation includes large numbers of particles and it is possible to assign groups of particles having similar initial conditions to distinct classes or 'parcels'. Each parcel is distinguished by common initial position and properties of its particles and the number of particles within it. The path of a given parcel can be represented by the path of a single constituent particle possessing the properties of that class. This allowed the specification of a parcel at each inlet cell which contained particles to be injected at each timestep. The effect of the dispersed phase on the continuum was calculated by using the coupled solution facility in STAR-CD [11].

The two phase computations were performed by introducing a parcel at each inlet cell loaded with 50000 solid particles. The particles were assumed to be spherical, with diameters of 3×10^{-7} m and 3×10^{-5} m analysed in separate computations.

Figure 7 shows a model with a domed top surface which is typical of the actual centrifugal rotor under investigation. The domed surface model was also used for a two-phase

computation and is the last model to be included for discussion.

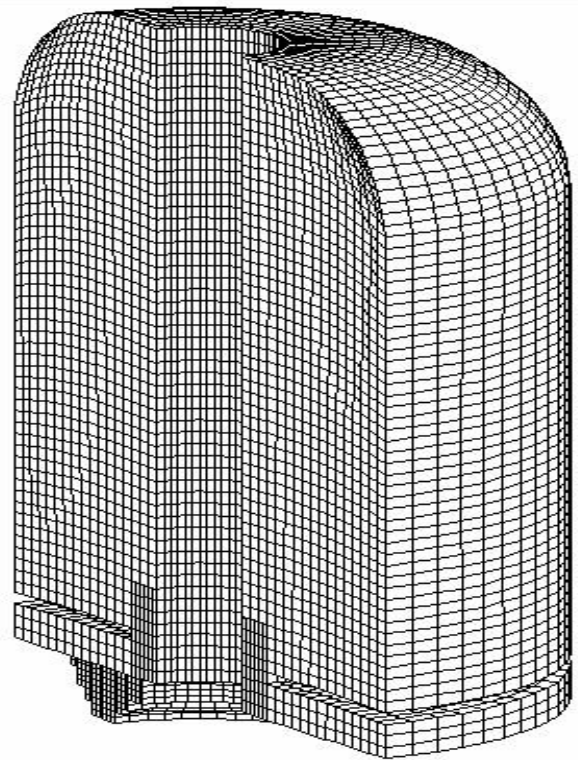


Figure 7. The Domed Top

RESULTS

The results from the basic model (Figure 1) with no through-flow but rotating at full speed showed the pressure distribution and tangential velocities to be in good agreement with the theoretical result for a fluid in solid body rotation, at any time sufficiently long after starting the rotation, due to the momentum imparted into the fluid from the walls of the rotor. This result confirms the model's ability to predict the characteristics of a fluid in rotation.

The inclusion of through-flow in addition to rotation showed that the inflow reduced slightly the tangential velocity of the fluid around the inlet but did not penetrate far radially into the rotor. The other main feature in this computation was a backflow of oil caused by flow in the outlet channel being forced back into the upper chamber of the rotor. This backflow causes some secondary flows within the rotor, resulting in a reduction in tangential velocity from that for solid body rotation. (The secondary flows also cause a reduction in the pressure gradient across the rotor radius.)

A separation disc is present in the actual rotor to stop any slumping of the contaminant cake from blocking the outlets. Results for the model with the separation disc included (Figure 6) showed similar characteristics to those described above, for example limited radial penetration and reduction in

tangential velocities near the inlet. However the separation disc did affect the flow-fields elsewhere in the rotor. Some backflow was still present but the majority was prevented from entering the upper chamber as most is deflected by the separation disc towards the outer radius of the rotor and confined to the outlet channel. A small amount of backflow still enters the upper chamber but not enough to cause disruptive secondary flow, resulting in tangential velocities in the upper chamber closer to those for solid body rotation at the rotor speed. The secondary flow is largely limited to the small bottom chamber which does not contribute to the separation of the contaminant.

The fluid near the inlet rotates at close to the operating speed. This limits the radial penetration of the inlet flow, which instead is directed axially up and (predominantly) down. This computed downwash of fluid has also been observed in flow visualisation experiments carried out at Bath (with water as the working fluid) using a perspex flat-top rotor bonded to the separation disc and base of a real rotor. Vegetable dye, injected into the inlet flow, was washed down the inner radius of the rotor. Limited amounts of backflow were also observed in these tests, but would have been difficult to interpret without the aid of computations.

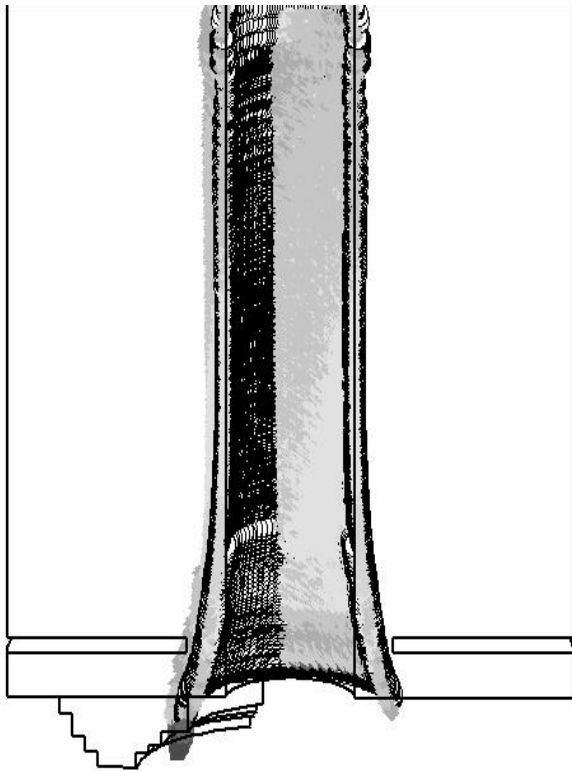


Figure 8. Downwash of Particles for $D_p = 3 \times 10^{-7} \text{m}$

Two-phase computations, using spherical particles of diameter $D_p = 3 \times 10^{-7} \text{m}$ ($0.3 \mu\text{m}$), showed that contaminant at this scale is washed with the inlet oil down the inner radius of

the rotor, as shown in Figure 8, a result which is consistent with the single phase results described above. Equation 1 shows that (at fixed operating conditions) small particles will be subject to a high retarding radial drag force compared with the modest centrifugal force at the inner radius (where r is small). As a result, the inlet momentum of very small particles is lost and these are carried by the secondary oil flow.

This computed result has been duplicated in experiments carried out by MANN+HUMMEL using a flat top rotor at the design speed and flow-rate [12]. A measured amount of the particulate material SoftC-2A (average diameter $0.7 \mu\text{m}$) was used to simulate contaminant found in the lube oil; this was found to wash through the rotor with no capture of particulates. MANN+HUMMEL rotors used in practice employ swept ribs in the rotor dome, as shown in Figure 1, to modify the flow-field in the vicinity of the inlet, giving rise to improved capture of small-scale contaminants.

A further computation was carried out for particles with diameter $D_p = 3 \times 10^{-5} \text{m}$ ($30 \mu\text{m}$). The downwash of fluid is present as before but these particles are centrifuged to the outer wall of the rotor, as shown in Figure 9. This demonstrates the relative reduction in the drag force, compared with the centrifugal force, indicated in equation 1 for the larger diameter particles.

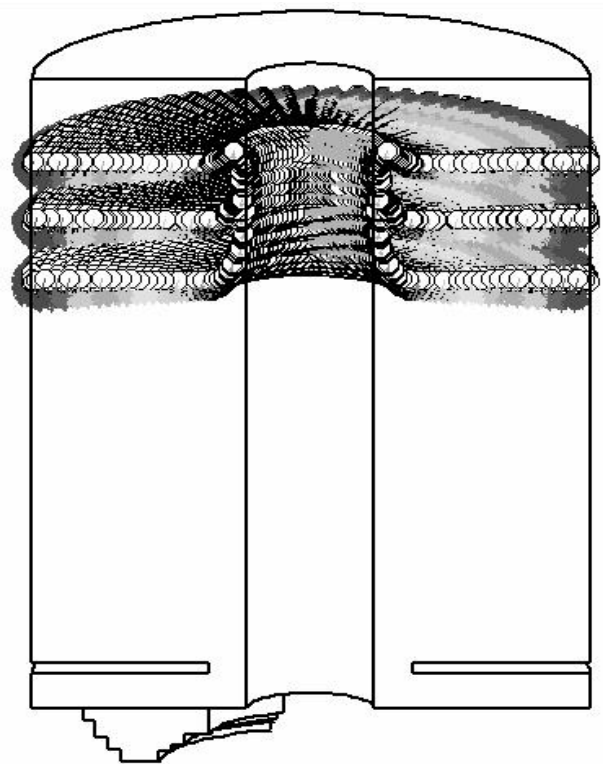


Figure 9. Centrifuged Particles, $D_p = 3 \times 10^{-5} \text{m}$

Computational results for the model with a domed top surface (Figure 7) mirrored those for the flat top geometry. The smaller particles were washed down the inner radius of

the rotor while the larger particles were again centrifuged to the outer wall. It is anticipated that the domed surface will have a more significant effect when ribs are also included in the model. This work is now in progress and will be described in due course.

CONCLUSIONS

By progressively increasing the features included in computations to investigate the flow characteristics within a sedimenting oil centrifuge, an understanding of the effects of different geometric and contaminant features has been gained.

The important yet unintended role of the separation disc in limiting backflow into the upper chamber of the rotor has been demonstrated by CFD which has been possible yet difficult to demonstrate with flow visualisation experiments. Tangential velocities were found to be close to solid body rotation, explaining the lack of penetration of the inlet flow and downwash of oil at the inner radius of the rotor.

Two-phase flow computations have complemented experiments carried out by MANN+HUMMEL, as both indicate that small particles (with diameters less than 10^{-6} m) are not subjected to the centrifuge effect but are carried in the downwash when using a rotor with a simplified geometry. This suggests that ribs used on the top of the actual rotor may play an important role by contributing to the mixing of fine particles, improving the effectiveness of sedimentation. The present research is continuing with the investigation of the effects of different rib and rotor top geometries on centrifugal sedimentation within the oil cleaning rotor.

ACKNOWLEDGEMENT

The computational work described here is part of a PhD research programme funded by MANN+HUMMEL.

REFERENCES

1. Cox I. M., Samways A. L. Diesel Engine Lube Oil Contamination Control Into The Next Millennium, MANN+HUMMEL (UK) Ltd, Chard, Somerset, UK
2. Heyward J. B., (1988) Internal Combustion Engine Fundamentals (International Edition), McGraw Hill, Singapore
3. Ishiguro T., Takatori Y., Akihama K., (1997), Microstructure of Diesel Soot Particles Probed by Electron Microscopy: First Observations of Inner Core and Outer Shell, January 1997, Vol. 108, No. 1, pp.231–234
4. Kawamura M., Ishiguro T., Morimoto H., (1987) Electron Microscope Observations of Soots in Used Diesel Engine Oils, Lubrication Engineering, July 1987, Vol. 43, No. 7, pp.572–575
5. Margaroni D., (1999) Extended Drain Intervals for Crankcase Lubricants, Industrial Lubrication and Tribology, Vol 51, No.2, May 1999, pp.69–76
6. Samways A. L., Cox I. M. (1998), A Method for Meaningfully Evaluating the Performance of a By-Pass Centrifugal Oil Cleaner, SAE Paper No.980872
7. Clague A. D. H., Donnet J. B., Wang T. K., Peng J. C. M. (1997), A Comparison of Diesel Engine Soot with Carbon Black, 1997, Vol. 37, No. 10, pp.1553–1565
8. Federal–Mogul Oil Conditioning Systems (1998), A Review of Soot in Lubricating Oil, March 1998, Federal–Mogul Oil Conditioning Systems, Illminster, Somerset, UK
9. Hsu H–W., (1981), Separations By Centrifugal Phenomena (1st Ed.), Techniques of Chemistry Vol. XVI, John Wiley & Sons Inc., New York,
10. Coombs P., Cox I. M., Samways A., (1998), Doubling Oil Drain Interval – The Reality of Centrifugal Bypass Filtration, May 1998 SAE Paper No. 981368
11. STAR–CD Methodology (1998), Version 3.05, Computational Dynamics Limited
12. Samways A. L. (2000), Private Communication MANN+HUMMEL (UK) Ltd, Chard, Somerset, UK

